Insulin signalling to mTOR mediated by the Akt/PKB substrate PRAS40

Emilie Vander Haar[1], Seong-il Lee[1], Sricharan Bandhakavi[1], Timothy J. Griffin[1] and Do-Hyung Kim[1,2]

Insulin stimulates protein synthesis and cell growth by activation of the protein kinases Akt (also known as protein kinase B, PKB) and mammalian target of rapamycin (mTOR). It was reported that Akt activates mTOR by phosphorylation and inhibition of tuberous sclerosis complex 2 (TSC2)[1–4]. However, in recent studies the physiological requirement of Akt phosphorylation of TSC2 for mTOR activation has been questioned[5,6]. Here, we identify PRAS40 (proline-rich Akt/PKB substrate 40 kDa) as a novel mTOR binding partner that mediates Akt signals to mTOR. PRAS40 binds the mTOR kinase domain and its interaction with mTOR is induced under conditions that inhibit mTOR signalling, such as nutrient or serum deprivation or mitochondrial metabolic inhibition. Binding of PRAS40 inhibits mTOR activity and suppresses constitutive activation of mTOR in cells lacking TSC2. PRAS40 silencing inactivates insulin-receptor substrate-1 (IRS-1) and Akt, and uncouples the response of mTOR to Akt signals. Furthermore, PRAS40 phosphorylation by Akt and association with 14-3-3, a cytosolic anchor protein, are crucial for insulin to stimulate mTOR. These findings identify PRAS40 as an important regulator of insulin sensitivity of the Akt–mTOR pathway and a potential target for the treatment of cancers, insulin resistance and hamartoma syndromes.

mTOR, a member of the phosphatidyl-inositol kinase-related protein kinase family, is an important regulator of the growth of mammals in response to the availability of nutrients, and is a key mediator of insulin, insulin-like growth factor 1 and other growth-factor signals to the cell growth machinery[7–9]. Hyperactivation of mTOR caused by abrogation of its negative regulators (such as phosphatase and tension homolog (PTEN) and TSC2) has been identified in a number of human cancers, including prostate cancers, multiple myeloma and several hamartoma syndromes (including TSC, Cowden's disease and Peutz-Jeghers syndrome[10,11]). Inhibition of mTOR in rodents and *Caenorhabditis elegans* has been shown to reduce insulin resistance, prevent tumorigenesis and TSC, and extend lifespan[12–14]. The broad implication of mTOR in many human diseases and physiological states is likely to be associated with

mTOR regulation by the insulin pathway. mTOR interacts with raptor (a scaffold protein that functions in recruiting mTOR substrates) and GβL (G-protein β-subunit-like protein; a regulator of mTOR kinase activity) to form mTORC1, a nutrient- and insulin-regulated complex[15–18], or with rictor and GβL to form mTORC2, which is involved in cytoskeleton regulation and Akt phosphorylation[19–21]. The mTOR complex containing raptor, mTORC1, has been considered an important interface through which insulin-regulated Akt signals are integrated with signals derived from nutrients.

Several studies have revealed that Akt activates mTORC1 through phosphorylation of TSC2 and subsequent activation of Rheb (Ras homolog enriched in brain), a positive regulator of mTOR[1–4]. However, recent studies using both mammalian cells and *Drosophila* showed that the physiological requirement of Akt phosphorylation of TSC2 for mTOR activation is unclear[5,6]. Furthermore, as yet, the interactions or post-translational modifications that occur in mTOR and its associated proteins (raptor, rictor and GβL) in response to insulin have not been identified. Although insulin does not change the interaction of mTOR with its associated proteins[16,17,19], currently unexplored properties of raptor, rictor and GβL, and other unidentified mTOR-binding effector proteins, may provide clues to the mechanism underlying insulin-regulated mTOR activation.

To identify additional proteins that modulate mTOR activity, we employed a mass spectrometry approach using an electrospray linear ion trap mass spectrometer (LTQ) combined with mTOR immunoprecipitation. mTOR immunoprecipitates were prepared from 293T cells using an mTOR antibody. Proteins bound to mTOR were eluted from the immunoprecipitates in a mild denaturing condition. Mixtures of proteins eluted from mTOR immunoprecipitates were trypsinized and mass spectra were obtained for peptides derived from the tryptic digestion of eluted proteins. MS/MS hits of peptides matched to mass spectra were analysed using the Sequest software[22] and scored with a P value[23], a parameter of fidelity for MS/MS matches. The highest P scores were obtained for peptides derived from tryptic digestion of raptor, rictor and GβL, demonstrating that this approach allows isolation of mTOR-binding proteins (see Supplementary Information, Table S1). We also identified three peptide sequences with high
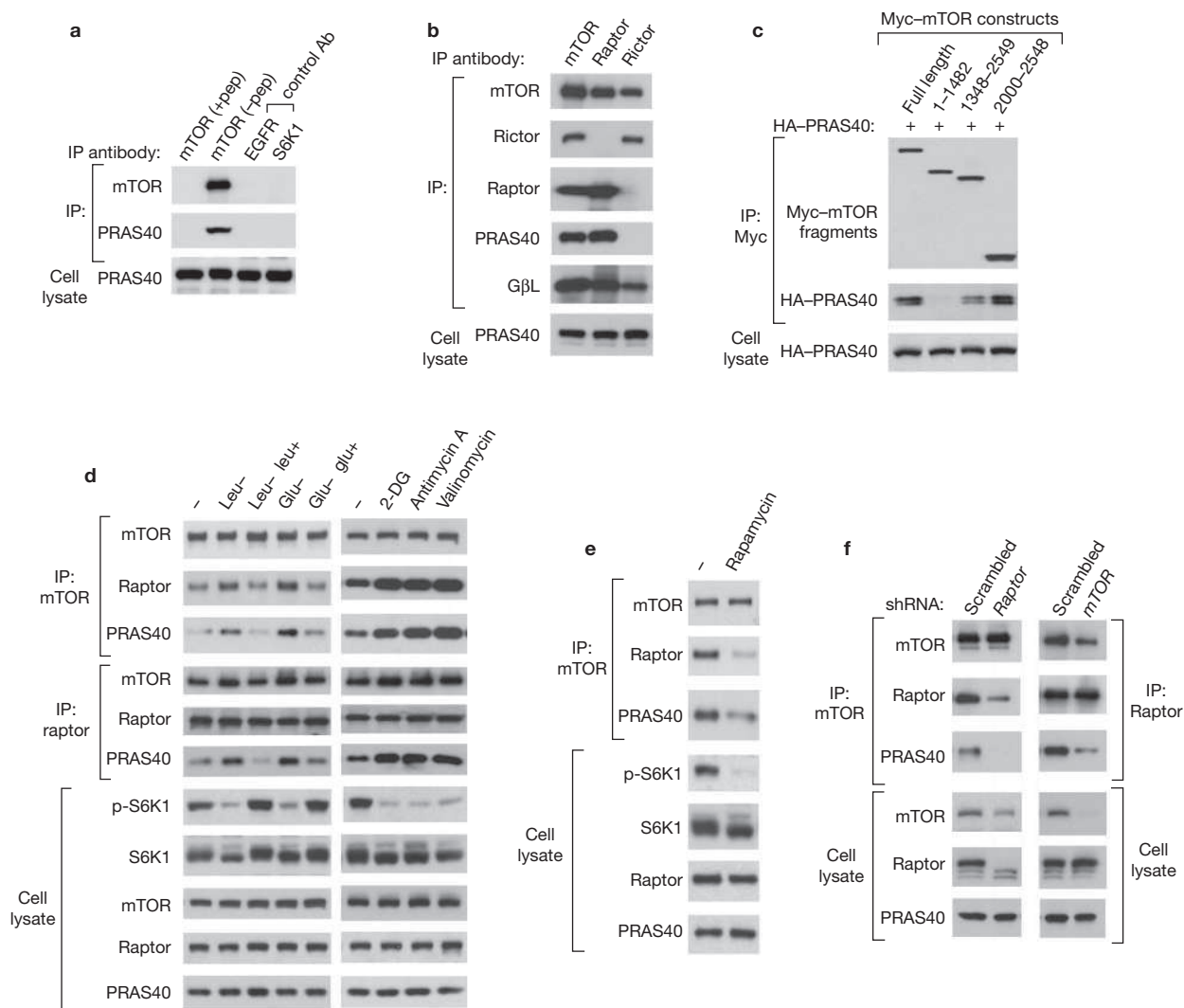
Figure 1 PRAS40 interacts with the raptor–mTOR complex. (**a**) mTOR immunoprecipates obtained from 293T cells in the presence (+pep) or absence (-pep) of mTOR antibody epitope peptides were analysed using a human PRAS40-specific monoclonal antibody on western blots. (**b**) PRAS40 is detected in mTOR and raptor immunoprecipitatesm but not in rictor immunoprecipitates. Anti-mTOR, raptor and rictor polyclonal antibodies were used for immunoprecipitation to isolate mTOR-, raptor- and rictor-binding proteins from 293T cells. (**c**) PRAS40 binds the mTOR kinase domain. The amount of HA–PRAS40 bound to Myc-tagged mTOR fragments expressed in 293T cells was analysed by immunoblotting. (**d**) PRAS40 binding to mTOR and raptor is stabilized by nutrient starvation and mitochondrial metabolic

inhibition in 293T cells. 293T cells were starved for leucine or glucose for 40 min and supplemented with leucine at 52 µg ml^{-1} or glucose at 11 mM for 10 min. Cells were also treated with indicated inhibitors at the concentrations of 100 mM 2-DG, 5 µM antimycin A or 1 µM valinomycin for 10 min. (**e**) Rapamycin disrupts the PRAS40–mTOR interaction. 293T cells were treated with rapamycin at 20 nM or a vehicle (–) for 20 min. (**f**) PRAS40 requires both mTOR and raptor for its association with the mTOR complex. 293T cells were transduced by a lentiviral shRNA specific to *mTOR* or raptor or a scrambled shRNA. Three days after the viral infection, the amounts of mTOR, raptor and PRAS40 in mTOR and raptor immunoprecipitates were analysed on immunoblots.

P scores from Sin1, a human orthologue of *S. cerevisiae* Avo1p that interacts with Tor2p in yeast[15]. We confirmed that Sin1 specifically interacts with mTOR and rictor in coimmunoprecipitation assays and determined that Sin1 has a crucial role in the formation of the rictor–mTOR interaction (see Supplementary Information, Fig. S1). The Sin1–mTOR interaction has also been identified in recent studies by other groups[24,25]. Additionally, a peptide sequence from PRAS40, a protein that is phosphorylated by Akt and binds 14-3-3 (ref. 26), was identified and is seemingly convserved in higher eukaryotes[27] (see Supplementary Information, Fig. S2). Because of the functional link between PRAS40 and Akt, we determined whether this protein is truly a binding partner of mTOR.

To confirm that mTOR specifically interacts with PRAS40, mTOR immunoprecipitates were obtained from HEK293T cells and the amount of endogenous PRAS40 in the immunoprecipitates was analysed by western blotting. PRAS40 was only detected in mTOR immunoprecipitates, but not in control immunoprecipitates. Furthermore, both endogenous and recombinant PRAS40 interacted with mTOR, but not with control proteins (Fig. 1a and see Supplementary Information, Fig. S3). Importantly, PRAS40 was detected in raptor immunoprecipitates, but not in rictor immunoprecipitates, suggesting that PRAS40 specifically targets mTORC1 (Fig. 1b). Supporting the hypothesis that a large proportion of the mTOR–raptor complex is regulated through its interaction with PRAS40, near stoichiometric amounts of Myc-tagged PRAS40, GβL and
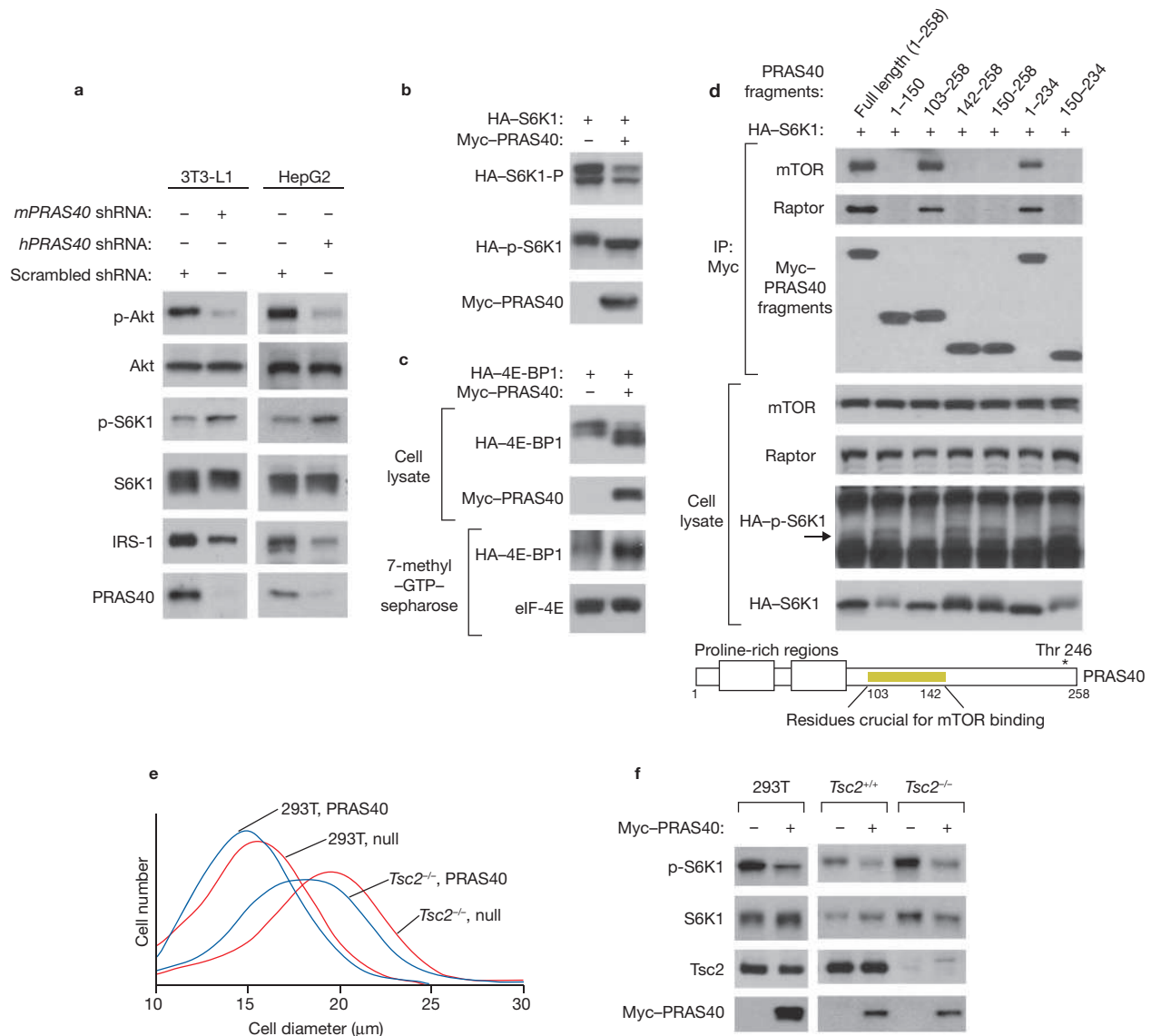
Figure 2 PRAS40 negatively regulates the mTOR pathway. (**a**) PRAS40 knockdown decreases IRS-1 levels, inhibits Akt phosphorylation and uncouples S6K1 phosphorylation from Akt signals. 3T3-L1 and HepG2 cells were transduced with a mouse or a human *PRAS40*-specific shRNA through lentiviral infection. As a control, a scrambled shRNA was used. The phosphorylation states of Akt at Ser 473 and S6K1 at Thr 389 and the expression levels of IRS-1, Akt, S6K1 and PRAS40 were analysed by immunoblotting. (**b**) PRAS40 overexpression inhibits S6K1 phosphorylation. HA-tagged S6K1 was expressed in 293T cells with or without Myc–PRAS40 and its phosphorylation state was analysed. (**c**) PRAS40 overexpression inhibits 4E-BP1 phosphorylation. HA–4E-BP1 was expressed in 293T cells with or without Myc–PRAS40 and the mobility on SDS–PAGE and

binding to 7-methyl-GTP sepharose resin of HA–4E-BP1 were analysed on immunoblots. (**d**) PRAS40 fragments capable of binding mTOR inhibit S6K1 phosphorylation. Immunoblots show the amounts of endogenous mTOR and raptor bound to PRAS40 fragments expressed in 293T cells and the phosphorylation state of HA–S6K1 coexpressed with PRAS40 fragments. (**e**) PRAS40 regulates size of cells. Myc-tagged human PRAS40 was expressed in 293T, EEF126-4 (*Tsc2*^{+/+}), and EEF126-8 (*Tsc2*^{-/-}) cells through lentiviral transduction. Cells that survived under zeocin-containing media were cultured at 20–30% confluence and analysed for cell sizes using the Beckman ViCell analyser. (**f**) Cells in **e** were harvested and the phosphorylation state of S6K1 and the expression levels of S6K1, *Tsc2* and Myc–PRAS40 were analysed by immunoblotting.

mTOR were observed crosslinked to HA–raptor in HA immunoprecipitates (see Supplementary Information, Fig. S3). Coimmunoprecipitation assays using mTOR fragments expressed in 293T cells showed that PRAS40 binds the mTOR carboxy-terminal kinase domain (Fig. 1c).

Interestingly, conditions that inhibit mTOR signalling (such as deprivation of leucine or glucose from the media, treatment with the glycolytic inhibitor 2-deoxyglucose and mitochondrial metabolic inhibitors such as valinomycin and antimycin) all led to an increase in the affinity of the PRAS40–mTOR interaction (Fig. 1d). Notably, this increase in affinity

requires raptor to be bound to mTOR, as lysis with Triton X-100 or treatment with rapamycin — both conditions that disrupt the raptor–mTOR interaction[16] — destabilized the PRAS40–mTOR interaction (Fig. 1e and see Supplementary Information, Fig. S3). Furthermore, either raptor or mTOR knockdown decreased the binding affinity of PRAS40 toward mTOR and raptor (Fig. 1f). These results demonstrate that raptor is important for the mTOR–PRAS40 interaction. The tightened association between the proteins under nutrient-starved conditions suggests a negative role for PRAS40 in the regulation of mTOR.
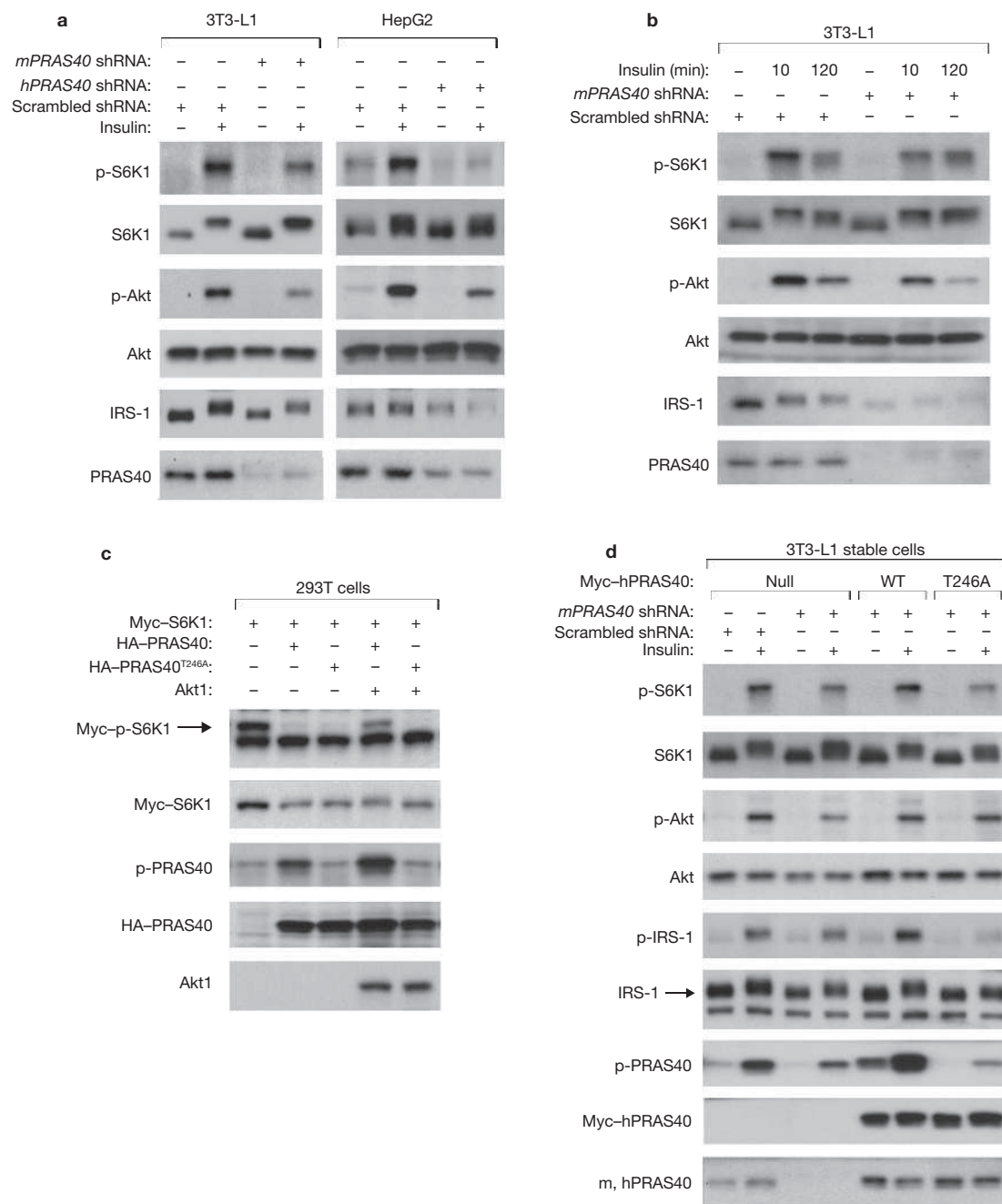
Figure 3 PRAS40 phosphorylation is crucial for insulin-regulated mTOR signalling. (**a**) PRAS40 knockdown inhibits insulin-stimulated phosphorylation of S6K1. PRAS40 or a scrambled shRNA was expressed in 3T3-L1 cells and HepG2 cells through lentiviral transduction. Forty-eight hours post-infection cells were starved of serum for one day and stimulated with 10 nM insulin for 20 min. (**b**) PRAS40 knockdown makes S6K1 phosphorylation insensitive to Akt. shRNA-transduced L1 cells were serum starved for 24 h and stimulated with 10 nM insulin for the indicated time. (**c**) PRAS40 phosphorylation at Thr 246 relieves S6K1 phosphorylation from the inhibition by PRAS40. Either wild-type PRAS40 or PRAS40^{T246A} was expressed in 293T cells with Akt and Myc–S6K1. Forty-eight hours post-transfection cell lysates were analysed for the phosphorylation states of S6K1 at Thr 389 and PRAS40 at Thr 246. (**d**) PRAS40 phosphorylation is important for mTOR activation by insulin. 3T3-L1 cells that stably express wild-type PRAS40 or PRAS40^{T246A} mutant were transduced by a lentiviral shRNA specific to mouse *PRAS40*. L1 cells stably transduced by null pCSII–EF–MCS vector were also infected with shRNA lentiviruses as controls. Forty-eight hours post-infection cells were starved of serum for 24 h and stimulated with 10 nM insulin for 10 min. Phosphorylated states and expression levels of indicated proteins were analysed by immunoblotting. Antibody specific to p-PRAS40 Thr 246 detects both human and mouse PRAS40 phosphorylated at Thr 246. The western blot labelled m, hPRAS40 (bottom panel) was obtained using a PRAS40 monoclonal antibody that detects both mouse and human PRAS40.

To investigate the functional consequence of the PRAS40–mTOR interaction in mTOR signalling, PRAS40 was downregulated in 3T3-L1 and HepG2 cells and the phosphorylation status of Akt at Ser 473 and S6K1 (a known substrate of mTOR) at Thr 389 was investigated. PRAS40 knockdown led to a dramatic decrease in Akt phosphorylation in both cell lines, indicating that PRAS40 silencing seems to have

negative effects on components upstream of Akt (Fig. 2a). Interestingly, this decrease in Akt phosphorylation was not accompanied by a decrease in S6K1 phosphorylation, but instead, elevated levels of S6K1 phosphorylation were observed in *PRAS40*-silenced cells. The result suggest that PRAS40-deprived mTOR complex can be active in S6K1 phosphorylation, even in conditions of low Akt activity, or that effects not mediated by Akt or mTOR are involved in the regulation of S6K1 phosphorylation. We investigated the mechanism underlying Akt inactivation induced by *PRAS40* silencing and found that levels of IRS-1, an upstream component of Akt, are highly decreased in *PRAS40*-silenced cells. This result indicates that *PRAS40* knockdown and the resulting activated state of mTOR may contribute to Akt inactivation through negative regulation of IRS-1 by mTOR and S6K1 — a feedback inhibition identified in several cell types[28].

We then analysed the effects of PRAS40 overexpression on mTOR activity. Consistent with the negative roles of PRAS40 in mTOR regulation, overexpression of PRAS40 in 293T cells decreased S6K1 phosphorylation (Fig. 2b) and enhanced the association of 4E-BP1 (another substrate of mTOR) with eukaryotic initiation factor 4E (eIF-4E) bound to 7-methyl-GTP affinity resin, an interaction that inhibits eIF-4E fucntion (Fig. 2c). Inhibition of S6K1 phosphorylation was only observed with overexpression of PRAS40 deletion constructs capable of binding mTOR and raptor in 293T cells, indicating that PRAS40 inhibition of mTOR activity is likely to require mTOR and raptor binding (Fig. 2d).

The negative regulation of mTOR by PRAS40 prompted us to examine whether PRAS40 can inhibit the hyperactive mTOR signalling in *TSC2*-silenced or Rheb-overexpressing cells. Consistent with a dominant-negative effect of PRAS40 on TSC–Rheb signalling, PRAS40 overexpression suppressed S6K1 phosphorylation in *TSC2*-silenced or Rheb-overexpressing 293T cells (see Supplementary Information, Fig. S3). PRAS40 overexpression also inhibited S6K1 phosphorylation in 293T cells expressing Rheb[Q64L], a constitutively active mutant, suggesting that PRAS40 acts downstream of, or in parallel with, Rheb in mTOR signalling. Consistent with an inhibitory effect of PRAS40 on mTOR-regulated cell growth, 293T cells and rat embryonic fibroblast cells EEF126-4 (*Tsc2*+/+) and EEF126-8 (*Tsc2*−/−) overexpressing PRAS40 were significantly smaller in cell volume and exhibited reduced levels of S6K1 phosphorylation compared with control cells without overexpressed PRAS40 (Fig. 2e, f and see Supplementary Information, Table S2).

Given the inhibitory function of PRAS40 in mTOR signalling, we wanted to determine the role PRAS40 plays in hormonal regulation of mTOR. *PRAS40* knockdown in mouse 3T3-L1 cells and human HepG2 cells impaired the ability of insulin to stimulate S6K1 phosphorylation at Thr 389 (Fig. 3a), supporting the possibility that PRAS40 may be necessary for insulin sensitization of mTOR signalling. *PRAS40* silencing reduces the levels of IRS-1 and Akt phosphorylation in both cell types. Serum starvation for 24 h completely suppressed S6K1 phosphorylation in *PRAS40*-silenced cells. This result supports an involvement of growth factor-regulated inputs, other than mTOR and PRAS40, in S6K1 phosphorylation. Furthermore, we observed that basal levels of S6K1 Thr 389 phosphorylation were higher in HepG2 control cells (Fig. 3a). This may be due to higher susceptibility of the control cells than *PRAS40*-silenced cells to growth factor or autocrine signals, even at a minimal levels.

To further investigate the requirement for PRAS40 in the response of mTOR to insulin, cells were treated with insulin for 2 h, a period sufficient to desensitize the cellular response to insulin as assessed by destabilization

of IRS-1 and reduced Akt phosphorylation. After this prolonged insulin treatment, *PRAS40*-silenced L1 cells failed to show a decrease in S6K1 phosphorylation relative to that of a 10 min treatment, whereas the scrambled short hairpin RNA (shRNA) cells showed a decrease in this phosphorylation (Fig. 3b). Consistent with our result showing an increase in S6K1 phosphorylation in *PRAS40*-silenced L1 and HepG2 cells (Fig. 2a), the level of S6K1 phosphorylation in *PRAS40*-silenced L1 cells after the prolonged insulin treatment was higher than in scrambled shRNA-transduced control cells (Fig. 3b). These data suggest that *PRAS40* silencing uncouples mTOR from Akt signals, further indicating a crucial role for PRAS40 in the regulation of Akt signalling to mTOR.

Because insulin stimulates Akt-mediated phosphorylation of PRAS40 at Thr 246 (ref. 26), we considered the possibility that PRAS40 phosphorylation may influence insulin activation of mTOR. Both wild-type PRAS40 and mutant PRAS40[T246A] expressed in 293T cells inhibited S6K1 phosphorylation and this inhibition was reduced on Akt1 coexpression with wild-type PRAS40 but not PRAS40[T246A] (Fig. 3c). To confirm the role of PRAS40 phosphorylation at Thr 246, 3T3-L1 stable cell lines expressing either wild-type human PRAS40 or PRAS40[T246A] in amounts comparable to physiological levels were generated. We knocked down endogenous mouse PRAS40 (known as Akt1s1) in the stable cells by transduction with lentiviral shRNA specifically targeting mouse PRAS40, but not human PRAS40, and investigated the insulin sensitivity of mTOR signalling. S6K1 phosphorylation was stimulated by insulin in wild-type cells to a similar extent to that in scrambled shRNA-transduced control cells, but the phosphorylation was highly suppressed in PRAS40[T246A]-expressing cells (Fig. 3d). Notably, wild-type cells exhibited an elevated level of mTOR-mediated phosphorylation of IRS-1 at Ser 636/Ser 639, a site known to be important for IRS-1 stability and insulin resistance[28]. In contrast, the level of IRS-1 phosphorylation was significantly lowed in PRAS40[T246A] cells, supporting the hypothesis that PRAS40 phosphorylation has a crucial role in the regulation of IRS-1 stability. Taken together, these findings demonstrate that Akt-mediated phosphorylation of PRAS40 is important for mTOR activation by insulin.

Next, we investigated the possibility that binding of PRAS40 to 14-3-3, an interaction induced on PRAS40 phosphorylation[26], may function in the activation of mTOR. S6K1 phosphorylation was relieved from PRAS40 inhibition in 293T cells when Myc-tagged 14-3-3 was coexpressed with wild-type PRAS40 but not with PRAS40[T246A], which is incapable of binding 14-3-3 (see Supplementary Information, Fig. S4). Expression of both myr–Akt1, a constitutively active form of Akt1, and 14-3-3 in 293T cells had a synergetic effect on S6K1 phosphorylation compared with expression of Akt1 or 14-3-3 alone. Furthermore, phosphorylation and binding to 14-3-3 of wild-type PRAS40 in 293T cells destabilized the interaction between PRAS40, mTOR and raptor (Fig. 4A). Consistent with a lower binding affinity of the PRAS40–14-3-3 complex for mTOR, insulin decreased the amount of PRAS40 bound to mTOR, and wortmannin, a PtdIns-3-kinase inhibitor, reversed this effect (Fig. 4B). These results imply that the PRAS40–14-3-3 complex may be dissociated from mTOR or weakly interact with mTOR, allowing recovery of mTOR activity from PRAS40 inhibition (Fig. 4C). PRAS40[T246E] and PRAS40[T246D], two phosphomimetic mutants, did not show any positive effects on S6K1 phosphorylation, either in the presence or absence of coexpressed Akt1 (see Supplementary Information, Fig. S4). The mutant proteins could not bind 14-3-3, further indicating that PRAS40–14-3-3 interaction is important for mTOR activation.
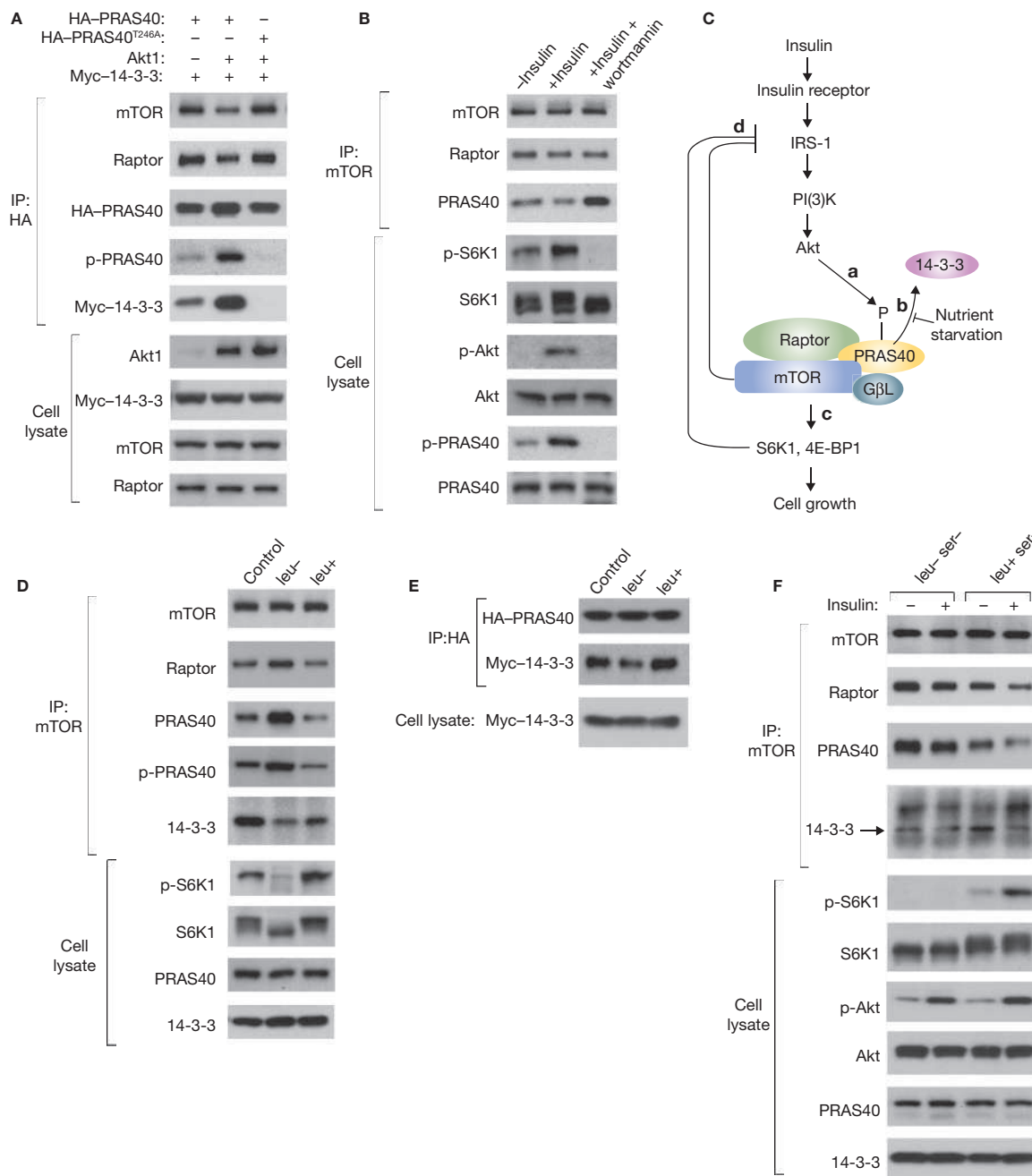
Figure 4 Insulin and nutrients regulate the PRAS40–mTOR interaction. (**A**) PRAS40 phosphorylation by Akt and binding to 14-3-3 destabilize the interaction between PRAS40, mTOR and raptor. HA-tagged wild-type PRAS40 or PRAS40[T246A] and Myc–14-3-3 were overexpressed, with or without Akt1, in 293T cells and the amounts of mTOR, raptor and Myc–14-3-3 in HA immunoprecipitates were determined on immunoblots. (**B**) Insulin destabilizes the interaction between mTOR and PRAS40. 293T cells were starved of serum for 24 h and treated with 100 nM insulin for 20 min or pretreated with 200 nM wortmannin for 10 min before the insulin treatment. mTOR immunoprecipitates were analysed to determine the amounts of PRAS40 bound to mTOR. (**C**) Schematic representation of a model explaining how PRAS40 interacts with mTOR and 14-3-3 in response to nutrients and insulin. The molecular processes that occur in response to insulin in the order are labelled a–d: a, Akt phosphorylation of PRAS40 at Thr 246; b, interaction with 14-3-3 and dissociation of PRAS40 from mTOR or loose association of PRAS40 with mTOR; c, recovery of mTOR activity from PRAS40 inhibition; d, negative-feedback inhibition of IRS-1 by mTOR and S6K1. (**D**) Nutrient starvation increases the affinity of the PRAS40–mTOR interaction and inhibits PRAS40 interaction with 14-3-3. 293T cells were not treated (control), deprived of leucine for 1 h (leu–), or cultured in the leu– media supplemented with leucine (52 μg ml^{–1}) for 1 h. The leucine minus and plus media contained 10% dialyzed fetal bovine serum. Endogenous PRAS40 and 14-3-3 isolated in mTOR immunoprecipitates were detected on immunoblots. (**E**) 293T cells expressing HA–PRAS40 and Myc–14-3-3 were incubated in leucine-deprived or -supplemented media as in **D** and the amount of Myc–14-3-3 bound to HA–PRAS40 was analysed. (**F**) Leucine starvation inhibits insulin-induced destabilization of the PRAS40–mTOR interaction. 293T cells were serum starved for 24 h and incubated in leucine- and serum-deprived media (leu–, ser–) or in the leu–, ser– media supplemented with leucine (leu+, ser–) for 1 hour before insulin treatment (100 nM) for 10 min. mTOR immunoprecipitates were analysed to detect the amount of PRAS40 and 14-3-3 bound to mTOR on immunoblots.

A model consistent with our results postulates PRAS40 as a crucial mediator of Akt signals to mTOR. On Akt activation by insulin, PRAS40 is phosphorylated at Thr 246 and binds 14-3-3. The 14-3-3 binding may lead to facilitated release of PRAS40 from mTOR, or loose association of PRAS40 with mTOR, to activate mTOR and to inactivate IRS-1 through the negative feedback regulation. Because insulin cannot activate mTOR when amino acids or glucose are limited in supply[7–9], we questioned whether nutrient starvation can influence the association of PRAS40 with mTOR under insulin stimulation. Supporting that nutrient starvation has dominant effects on the mTOR–PRAS40 interaction over growth factor stimulation, PRAS40 was barely released from mTOR under a leucine-deprived condition compared with a leucine-supplemented condition, despite high serum levels (Fig. 4D). Furthermore, the amount of 14-3-3 bound to mTOR and PRAS40 was highly reduced under leucine-deprived conditions, indicating that the interaction between 14-3-3 and PRAS40 is prevented under the nutrient-starvation condition (Fig. 4D, E). Confirming this result, insulin-stimulated release of PRAS40 from mTOR and PRAS40 binding to 14-3-3 were prevented when cells were cultured under leucine-deprived conditions (Fig. 4F).

Our results support the hypothesis that PRAS40 is not only a key mediator of Akt signals to mTOR, but is also a dominant-negative effector of mTOR over TSC–Rheb signalling. We demonstrated that PRAS40 is an important regulator of IRS-1 stability and insulin sensitivity of mTOR signalling, suggesting a potential role for PRAS40 in insulin resistance. PRAS40 was also shown to be important in carcinogenesis[29] and neuronal cell death[30]. Although we identify an inhibitory role of PRAS40 for mTOR signalling, we do not exclude the possibility that PRAS40 functions as a scaffold protein that recruits mTOR effectors. The proline-rich regions in the amino-terminal half of PRAS40 may serve as binding sites for proteins containing Src homology 3 (SH3) and WW, or help assemble multi-element signalling complexes. Future studies involving PRAS40 regulation of mTOR may increase our knowledge of cancer, neuronal disease, insulin resistance and several hamartoma syndromes. □

METHODS

Reagents and antibodies. Anti-mTOR (sc-1549), anit-EGFR (sc-31157), anti-TSC2 (sc-893) and anti-14-3-3 (sc-732) antibodies were purchased from Santa Cruz Biotech (Santa Cruz, CA). Anti-PRAS40 monoclonal antibody specific to human PRAS40 (AHO1031), anti-phospho-PRAS40 polyclonal antibody (44-1100G), and a monoclonal antibody specific to human and mouse PRAS40 (NON0684) were obtained from Invitrogen (Carlsbad, CA). Raptor-, rictor- and Sin1-specific antibodies were generated against peptide sequences, MESEMLQSPLLGLGEEDEAD, RGRSLKNLRVRGRND and TDFPPLDSNEPIHK, respectively, as epitopes from Invitrogen custom antibody service. Anti-Myc 9E10 was purchased from EMD Biosciences (San Diego, CA) and antibodies against S6K1 (9202), phospho-S6K1 Thr 389 (p-S6K1; 9205), Akt (9272), phospho-Akt Ser 473 (p-Akt; 9271), IRS-1 (2382), and phospho-IRS1 Ser 636/Ser 639 (p-IRS1; 2388) were from Cell Signaling Tech. (Danvers, MA). Anti-HA antibody (HA.11) was from Covance (Berkeley, CA). Porcine insulin and wortmannin were purchased from Sigma-Aldrich (St Louis, MO) and EMD Biosciences (San Diego, CA), respectively, and 4E-BP1 was from Stratagene (La Jolla, CA). Wild-type HA–Akt and myr–AKT1–Myc clones were obtained from W. Sellers (Harvard University, Boston, MA) and Upstate (Chicago, IL), respectively. Glutathione-4B beads and 7-methyl-GTP sepharose resin were from GE Healthcare Bio-Sciences (Piscataway, NJ).

Plasmid constructions and mutagenesis. Human PRAS40 cDNAs were provided by R. Roth (Stanford University, CA) and the American Type Culture Collection (ATCC, Manassas, VA; Image# 2988648) and mouse PRAS40 cDNA obtained from ATCC (Image# 3487281) were cloned into prk5–Myc and prk5–HA expression vectors by use of a PCR amplification kit (Roche, Nutley, NJ). PRAS40 DNA fragments were generated by PCR amplification and subcloned into mammalian expression vector prk5–Myc and all the clones confirmed by sequencing. PRAS40 Thr 246 was replaced by alanine, glutatmate and aspartate using a site-directed mutagenesis kit (Stratagene) and mutated primers. pLKO shRNA vector (provided by S. Stewart, Washington University, MO) was used for knockdown experiments. Target sequences for human PRAS40 and TSC2 were 5′-CAGCTGGGCATTAGT-GATAAT-3′ and 5′-CACTGGCCTTGGACGGTATTG-3′, respectively, and for mouse PRAS40 was 5′-GAGCCCACTGAAACAGAGACA-3′. Target sequences for human mTOR, raptor, rictor and Sin1 were 5′-AACCCTGCCTTTGTCAT-GCCT-3′, 5′-CACCTCACTTTATTTCCATGT-3′, 5′-CACCACCAAAG-CAACCTATAG-3′ and 5′-TAGGTACAACAGCAACCAAGA-3′, respectively. A scrambled shRNA sequence, 5′-AACGTACGCGGAATACTTCGA-3′, was cloned as a control. The target sequence of the mouse PRAS40-specific shRNA (mPRAS40 shRNA) is completely matched to the mouse PRAS40 nucleotide sequence from 328 to 248 for 21 nucleotides, but mismatched to human PRAS40 sequence at six nucleotides. The mPRAS40 shRNA did not act at all on human PRAS40 in our test experiment. A lentiviral expression vector CSII–EF–MCS, kindly provided by N. Somia (University of Minnesota, MN), was used to express Myc–PRAS40 in HEK293T, HepG2, Eker rat embryonic fibroblast (EEF) Tsc2^{+/+} and EEF Tsc2^{–/–} cells. Myc–PRAS40 DNA construct was PCR-amplified and subcloned into the lentiviral vector. All other constructs used in the experiments have been previously described[16,17].

Identification of mTOR-interacting proteins. mTOR immunoprecipitates were prepared from 293T cells cultured in 10% fetal bovine serum-supplemented DMEM using an mTOR antibody (N19, Santa Cruz Biotech.). Cells were lysed in a buffer containing 40 mM HEPES at pH 7.4, 120 mM NaCl, 1 mM EDTA, 50 mM NaF, 1.5 mM Na$_3$VO$_4$, 10 mM β-glycerophosphate, 0.3% Chaps and EDTA-free protease inhibitors (Roche). Cell lysate from a 10-cm plate was incubated with 20 μl of protein G resin (20399; Pierce; Rockford, IL) and 4 μg of mTOR antibody for 3 h at 4 °C. As a control, an epitope peptide for the mTOR antibody was added during the immunoprecipitation. mTOR immunoprecipitates were washed four times with the lysis buffer. mTOR-binding proteins were eluted from the immunoprecipitate by incubating with 0.075% SDS. The eluate was diluted with a trypsin digestion buffer (25 mM sodium bicarbonate, 2.5 mM CaCl$_2$ at pH 8.0) and incubated with trypsin overnight. The trypsinized sample was diluted with 0.1% trifluoroacetic acid to obtain a pH below 3.0 and loaded onto a mixed-mode cation exchange cartridge (MCX cartridge; Waters Inc., Milford, MA) to remove salt and detergent from the samples. Peptides bound to the resin were eluted with 5% ammonium hydroxide in methanol and lyophilized. Lyophilized samples were dissolved in 0.1% formic acid and analysed by microcapillary electrospray tandem mass spectrometry (MS/MS) on an LTQ mass spectrometer (Thermo Electron, Milford, MA). MS/MS spectra were searched using Sequest software (Thermo Electron) against a non-redundant human protein sequence database (IPI human sequence database, version 3.0). Peptide sequence matches were filtered using a probabilistic scoring algorithm called Peptide Prophet[22,23], which assigns a value between zero and one to peptide sequence matches, with a score of one representing the highest confidence match. In this study, matches with a P score of 0.95 or greater were considered to be correct.

Cell culture and transfection. HEK293T, HepG2 and 3T3-L1 cells were cultured in DMEM (Invitrogen) supplemented with 10% fetal bovine serum, penicillin and streptomycin at 37 °C in 5% CO$_2$. F-12/DMEM (Invitrogen) was used to culture EEF cells. For transient expression, HEK293T cells were transfected with recombinant DNAs or shRNA plasmids using Fugene 6 (Roche) following the manufacturer's protocol. Cells were harvested two days post-transfection for the coimmunoprecipitation assays.

Coimmunoprecipitation and western blotting. For coimmunprecpititation studies, whole-cell extracts were prepared in 0.3% Chaps buffer and immunoprecipitated with anti-mTOR, anti-raptor, anti-rictor, anti-HA or anti-Myc antibodies. Precipitated proteins were washed four times in 0.3% Chaps buffer, loaded onto 8% Tris–glycine gels (Invitrogen), transferred for 4 h onto immunoblot polyvinylidene difluoride (PVDF) membranes (Bio-Rad, Hercules, CA) and detected with ECL western blotting detection reagents (Perkin-Elmer, Wellesley, MA).

Chemical crosslinking. For chemical crosslinking experiments, HEK293T cells were treated with dithiobis[succinimidylpropionate](Pierce) at a concentration of 0.5 mg ml^{-1} for 20 min and unreacted DSP was inactivated by 0.1 M Tris at pH 7.4. DSP-treated cells were harvested and lysed in a buffer containing 1% Triton X-100, 40 mM HEPES as pH 7.4, 120 mM NaCl, 1 mM EDTA, 50 mM NaF, 1.5 mM Na$_3$VO$_4$ and 10 mM β-glycerophosphate. Immunoprecipitates obtained from the cell lysate were incubated with 0.1 M DTT for 20 min at room temperature before analysis by SDS–PAGE.

Lentiviral preparation, viral infection and stable cell line generation. The CSII–EF–MCS lentiviral vector encoding Myc–PRAS40 was transfected into 293T cells with lentiviral packaging vectors ΔNRF–HIV-1–gag–pol (provided by N. Somia) and pCMV–VSV-G (provided by S. Stewart) using Fugene 6, and viruses were collected from the media 60 h post-transfection. Target cells grown on 6-cm dishes were infected with collected viruses four times over 15 h in the presence of polybrene (Sigma-Aldrich). The *pLKO* shRNA vectors encoding shRNAs that target *PRAS40* or scrambled sequences were transfected into HEK293T cells with lentiviral packaging vectors pHR'8.2ΔR and pCMV–VSV-G using Fugene 6. Viruses were collected 60 h after transfection, and 3T3-L1 cells and HepG2 cells were infected with the collected viruses four times over 15 h in the presence of polybrene. 3T3-L1 cells that stably expressed Myc-tagged wild-type human PRAS40 or PRAS40^{T246A} were generated by infecting L1 cells with lentiviruses. Individual cell colonies were selected and isolated in the presence of zeocin at the concentration of either 50 or 100 μg ml^{-1} two weeks after the viral infection and transferred to 24-well plates. Expression levels of Myc–PRAS40 in stable cell lines were analysed on western blots using anti-Myc and anti-PRAS40 monoclonal antibodies. Cells expressing Myc–PRAS40 at a level comparable to that of endogenous PRAS40 in 3T3-L1 cells were used for experiments. Selected cell lines were infected by shRNA lentiviruses to knockdown endogenous mouse *PRAS40* and selected in the presence of puromycin.

Cell-size measurement. HEK293T and EEF cells infected with lentiviruses and selected in the presence of zeocin were split into 6-cm plates at 20% confluence and the next day, cells were trypsinized and diluted ten times with DMEM. One ml of diluted cell culture was loaded on a ViCell cell-size analyser (Beckman Coulter Inc., Fullerton, CA).

Note: Supplementary Information is available on the Nature Cell Biology website.

COMPETING FINANCIAL INTERESTS
The authors declare that they have no competing financial interests.

1. Inoki, K., Li, Y., Zhu, T., Wu, J. & Guan, K. L. TSC2 is phosphorylated and inhibited by Akt and suppresses mTOR signalling. *Nature Cell Biol.* **4,** 648–657 (2002).
2. Manning, B. D., Tee, A. R., Logsdon, M. N., Blenis, J. & Cantley, L. C. Identification of the tuberous sclerosis complex-2 tumor suppressor gene product tuberin as a target of the phosphoinsitide 3-kinase/Akt pathway. *Mol. Cell* **10,** 151–162 (2002).
3. Zhang, Y. *et al.* Rheb is a direct target of the tuberous sclerosis tumour suppressor proteins. *Nature Cell Biol.* **5,** 578–581 (2003).
4. Long, X., Lin, Y., Ortiz-Vega, S., Yonezawa, K. & Avruch, J. Rheb binds and regulates the mTOR kinase. *Curr. Biol.* **15,** 702–713 (2005).
5. Dong, J. & Pan, D. J. Tsc2 is not a critical target of Akt during normal *Drosophila* development. *Genes Dev.* **18,** 2479–2484 (2004).
6. Hahn-Windgassen, A. *et al.* Akt activates the mammalian target of rapamycin by regulating cellular ATP level and AMPK activity. *J. Biol. Chem.* **280,** 32081–32089 (2005).
7. Brunn, G. J. *et al.* Phosphorylation of the translational repressor PHAS-I by the mammalian target of rapamycin. *Science* **277,** 99–101 (1997).
8. Dennis, P. B. *et al.* Mammalian TOR, a homeostatic ATP sensor. *Science* **294,** 1102–1105 (2001).
9. Shimji, A. F., Nghiem, P. & Schreiber, S. L. Integration of growth factor and nutrient signaling: implications for cancer biology. *Molecular Cell* **12,** 271–280 (2003).
10. Gao, X. *et al.* Tsc tumour suppressor proteins antagonize amino-acid-TOR signalling. *Nature Cell Biol.* **4,** 699–704 (2002).
11. Corradetti, M. N. Inoki, K., Bardeesy, N., Depinho, R. A. & Guan, K. L. Regulation of the TSC pathway by LKB1: evidence of a molecular link between tuberous sclerosis complex and Peutz-Jeghers syndrome. *Genes Dev.* **18,** 1533–1538 (2004).
12. Um, S. H. *et al.* Absence of S6K1 protects against age- and diet-induced obesity while enhancing insulin sensitivity. *Nature* **431,** 200–205 (2004).
13. Kenerson, H., Dundon, T. A. & Yeung, R. S. Effects of rapamycin in the Eker rat model of tuberous sclerosis complex. *Pediatr Res.* **57,** 67–75 (2005).
14. Vellai, T. *et al.* Genetics: influence of TOR kinase on lifespan in *C. elegans. Nature* **426,** 620 (2003).
15. Loewith, R. *et al.* Two TOR complexes, only one of which is rapamycin sensitive, have distinct roles in cell growth control. *Mol. Cell* **10,** 457–468 (2002).
16. Kim, D.-H. *et al.* mTOR interacts with raptor to form a nutrient-sensitive complex that signals to the cell growth machinery. *Cell* **110,** 163–175 (2002).
17. Kim, D.-H. *et al.* GβL, a positive regulator of the rapamycin-sensitive pathway required for the nutrient-sensitive interaction between raptor and mTOR. *Mol. Cell* **11,** 895–904 (2003).
18. Hara, K. *et al.* Raptor, a binding partner of target of rapamycin (TOR), mediates TOR action. *Cell* **110,** 177–189 (2002).
19. Sarbassov, D. D. *et al.* Rictor, a novel binding partner of mTOR, defines a rapamycin-insensitive and raptor-independent pathway that regulates the cytoskeleton. *Curr. Biol.* **14,** 1296–1302 (2004).
20. Sarbassov, D. D., Guertin, D. A., Ali, S. M. & Sabatini, D. M. Phosphorylation and regulation of Akt/PKB by the rictor-mTOR complex. *Science* **307,** 1098–1101 (2005).
21. Jacinto, E. *et al.* Mammalian TOR complex 2 controls the actin cytoskeleton and is rapamycin insensitive. *Nature Cell Biol.* **6,** 1122–1128 (2004).
22. Eng, J., McCormack, A. L. & Yates, J. R. An approach to correlate tandem mass spectral data of peptides with amino acid sequences in a protein database. *J. Am. Mass Spectrom.* **5,** 976–989 (1994).
23. Keller, A., Nesvizhskii, A. I., Kolker, E. & Aebersold, R. Empirical statistical model to estimate the accuracy of peptide identifications made by MS/MS and database search. *Anal. Chem.* **74,** 5383–5392 (2002).
24. Frias, M. A. *et al.* mSin1 is necessary for Akt/PKB phosphorylation, and its isoforms define three distinct mTORC2s. *Curr. Biol.* **16,** 1–6 (2006).
25. Jacinto, E. *et al.* Sin1/Mip1 maintains rictor-mTOR complex integrity and regulates Akt phosphorylation and substrate specificity. *Cell* **126,** 1–13 (2006).
26. Kovacina, K. S. *et al.* Identification of a proline-rich Akt substrate as a 14-3-3 binding partner. *J. Biol. Chem.* **278,** 10189–10194 (2003).
27. Singh, A., Chan, J., Chern, J. J. & Choi, K.-W. Genetic interaction of lobe with its modifiers in dorsoventral patterning and growth of the *Drosophila* eye. *Genetics* **171,** 169–183 (2005).
28. Tzatsos, A. & Kandror, K. V. Nutrients suppress phosphatidylinositol 3-kinase/Akt signaling via raptor-dependent mTOR-mediated insulin receptor substrate 1 phosphorylation. *Mol. Cell. Biol.* **26,** 63–76 (2006).
29. Huang, B. & Porter, G. Expression of proline-rich akt-substrate PRAS40 in cell survival pathway and carcinogenesis. *Acta. Pharmacol. Sin.* **26,** 1253–1258 (2005).
30. Saito, A. *et al.* Neuroprotective role of a proline-rich Akt substrate in apoptotic neuronal cell death after stroke: relationships with nerve growth factor. *J. Neurosci.* **24,** 1584–1593 (2004).

Figure S1

Figure S1. Sin1 is a component of mTORC2. (**a**) Sin1 is detected only in mTOR immunoprecipitates but not in control immunoprecipitates obtained using anti-EGFR or 14-3-3 antibodies or using anti-mTOR antibody in the presence of mTOR antibody epitope peptides (+pep). Two isoforms of Sin1 were detected to interact with mTOR on Western blots. Immunoprecipiates were obtained from HEK293T cells. (**b**) Sin1 is detected in mTOR and rictor immunoprecipitates but not in raptor immunoprecipitates obtained from 293T cells. (**c**) Recombinant Sin1 tagged with HA at the N-terminus interacts with endogenous mTOR. HA-Sin1 was overexpressed in 293T cells and the amount of mTOR bound to HA-Sin1 in HA immunoprecipitate was analyzed by Western blotting. HA-S6K1 was used as a control protein. (**d**) Sin1 is important for the rictor-mTOR interaction. Reciprocally, rictor is important for the Sin1-mTOR interaction. HeLa cells transduced by lentiviral shRNA targeting rictor or Sin1 were generated and cultured in the presence of puromycin. As a control, scrambled shRNA-transduced HeLa cells were used. mTOR immunoprecipitate was obtained from these cells and the amounts of rictor, raptor, and Sin1 bound to mTOR were analyzed by Western blotting.

Figure S2

```
                                                                                                                                                    Identity
                                                                                                                                                    similarity
H.sapiens 123 SDNGGLFVMDEDATLQDLPPFCESDPE-STDDGSLSEETPAGPPTCSVPPASALPTQQYAKSLPVSVPVWGFKEKRTEARSSDEENGPPSSPDLDRIAASMRALVLREAEDTQVFGDLPRPRLNTSDFQKLKRKY 256
              SD+ GLFVMDED+  QD  PF ESD E STDDGSL+++ P  PP    P +    QQYA+SLPV+VPVWGFKEK+ + +SSD+E       SPDLDRIAASMRAL +   + +Q FGDLPRPRLNT DFQ   RKY      60%,71%
X.laevis  154 SDSAGLFVMDEDSNSQDCEPFFESDQEESTDDGSLTDDLPGHPP----PQRNY---QQYARSLPVTVPVWGFKEKKQQNKSSDDETSKFPSPDLDRIAASMRALTI---DHSQPFGDLPRPRLNTGDFQTKYRKY 278

H.sapiens 127 GLFVMDEDATLQDLPPFCESD-PESTDDGSLSEETPAGPPTCSVPPASALPTQ--QYAKSLPVSVPVWGFKEKRTEARSSDEENGPP-SSPDLDRIAASMRALVLREAED-TQVFGDLPRPRLNTSDF 249
              G+F MDED+ +D  PF ESD  E + DGSLSEE P  ++  ++  +   A+SLPVSVPVWG++     A   D  +G     DLD IAASM+AL++  A D T++FG LPRPRLNT DF        44%,61%
D.rerio   220 GVFSMDEDSLSRDCEPFFESDGEEESTDGSLSEEAPPPRGMAMGHLASRSSNPMSMARSLPVSVPVWGYRN--NHAPQGDSHSGERVGCADLDHIAASMKALLVPGATDGTEMFGALPRPRLNTGDF 345

H.sapiens          147 DPESTDDG--SLSEETPAGPPTCSVPPASALPTQQYAKSLPVSVPVWGFKEKRTEARSSDEENGPPSSPDLDRIAASMRALVLREAEDTQVFGDLPRPRLNT 246
                       D E+ D+  +L ++   P    S    +A+SLP+ +    E+  A +++  G   D  IAAS++AL  R      VFGDLPRPRL              30%,46%
D.melanogaster Lobe 461 DDEAADEAEDALDPDSSISIPVRGGGRPSHAQLMNFARSLPIEIANTTLAERAAVANNNNFGQGCEEGMDNIDIAASIQALT-RSVHGEAVFGDLPRPRLRS 558

H.sapiens    182 AKSLPVSVPVW-GFKEKRTEARSSDEENGPPSSPDLDRIAASMRALVLREAEDTQVFGDLPRPRLNT 246
                 AKSLPVSVP +  F + ++ D+ +  P  P    I AS++AL     DT VFGDLPRPR +T        44%,58%
A.mellifera  332 AKSLPVSVPSFPSFVRRTVQDQDDDQLSRDPHDPH--NIRASIKALAKSVHGDT-VFGDLPRPRFST 395

H.sapiens   140 LPPFCESDPESTDDGSLSEETPAGPPTCSVPPASALPTQQYAKSLPVSVPVWGFKEKRTEARSSDEENGPPSSPDLDRIAASMRALVLREAEDTQVFGDLPRPRLNTS D 248
                + P +   S+DD S  E+ PA  PT    PA A P   AK       K   +  SSD+E  P + L ++A  +    +             + +S D          25%,37%
C. briggsae 238 MAPAAKKAASSSDDSSDDEKKPAAKPT----PAKATPKAPVAK----------KAASSSDDSSDDEKKPAAKPTLAKVASDDEKKPAAKPTPAKVAPKAPAAKKAASSSD 302
```
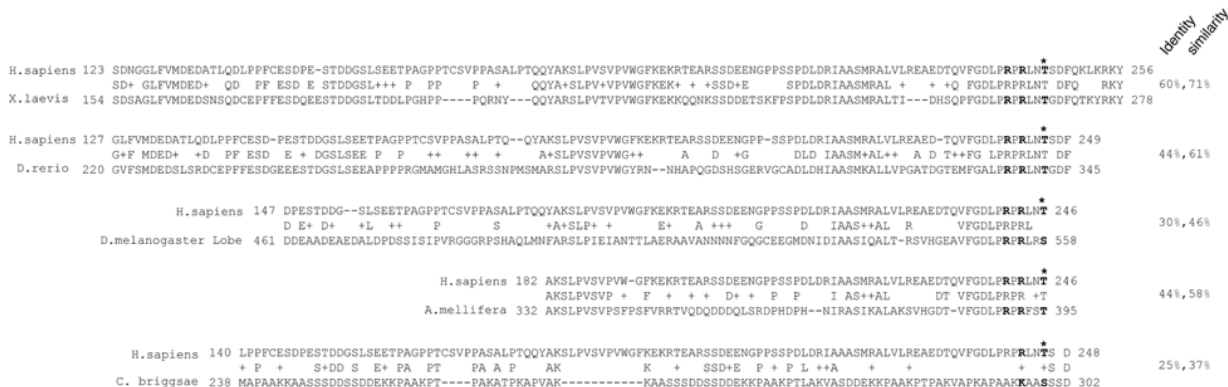
Figure S2. Sequence comparison between *H. sapiens* PRAS40 and proteins from other species. Blast searches revealed that 88-98% amino acids are identical between human PRAS40 and its homologues from other mammals. Unnamed proteins from *X. laevis*, *D. rerio*, *A. mellifers*, and *C. briggsae* and Lobe from *D. melanogaster*, a protein involved in the fly eye growth and development[27], were identified to have high sequence similarity with the C-terminal half of the human PRAS40, a region determined to bind mTOR. Residues in an Akt-phosphorylation consensus motif are in bold type. Threonine or serine labeled by an asterisk is an Akt-phosphorylation site.
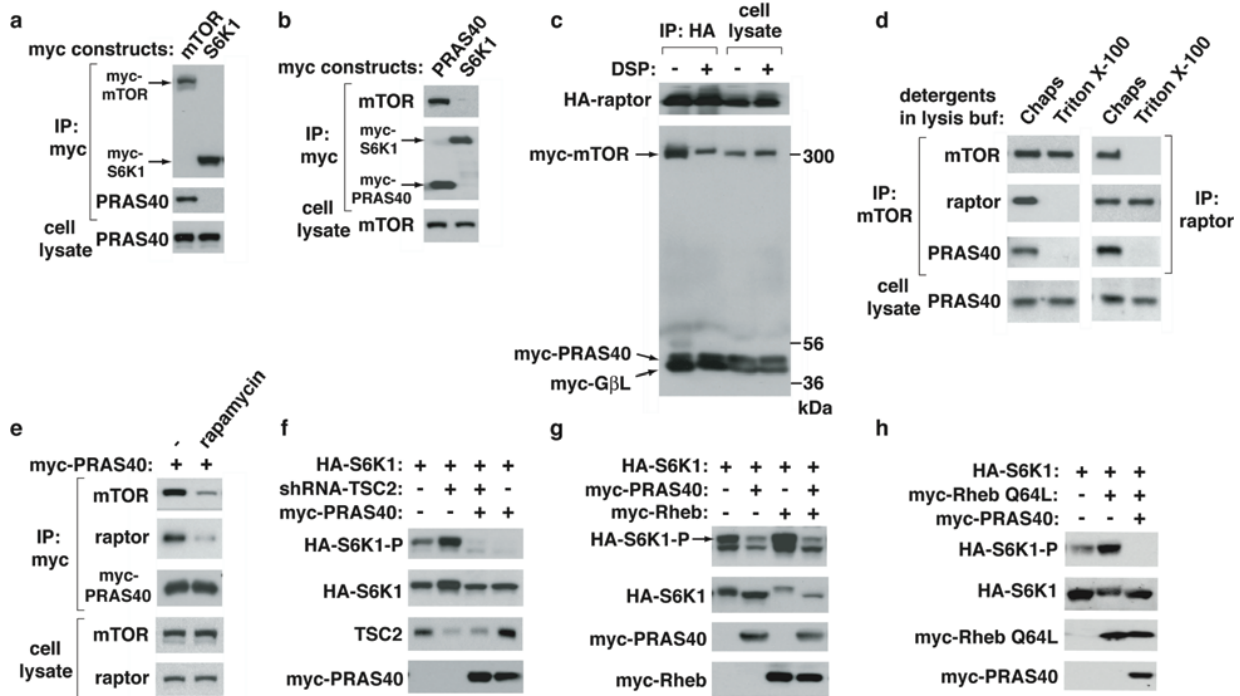
Figure S3

Figure S3. PRAS40 interacts with mTOR and raptor, and PRAS40 overexpression suppresses the increase of S6K1 phosphorylation induced by TSC2 silencing or Rheb overexpression. (**a**) Myc-tagged mTOR interacts with endogenous PRAS40 in 293T cells. The interaction was analyzed 48 hrs post-transfection. Myc-S6K1 was used as a control. (**b**) Myc-tagged PRAS40 interacts with endogenous mTOR in 293T cells. (**c**) Myc-tagged PRAS40, GβL, and mTOR in near stoichiometric amounts bind HA-raptor. 293T cells were transfected with plasmids encoding HA-raptor, myc-mTOR, myc-PRAS40, and myc-GβL. Two days post-transfection, 293T cells were lysed in a buffer containing 0.3% Chaps (-) or treated with DSP (Pierce) at the concentration of 0.5 mg/ml) for 20 min (+). DSP-treated cells were harvested and lysed in a buffer containing 1% Triton X-100 to remove proteins that were not crosslinked to mTOR. HA-raptor immunoprecipitate was isolated from harvested 293T cells and analyzed in the amount of myc-tagged mTOR, PRAS40, and GβL bound to HA-raptor on immunoblots. (**d**) PRAS40 requires both mTOR and raptor for binding the mTOR-raptor complex. mTOR and raptor immunoprecipitates were obtained from 293T cells lysed in a buffer containing Chaps or Triton-X100 and analyzed using a PRAS40 specific antibody. (**e**) Rapamycin disrupts the binding of PRAS40 to mTOR and raptor. Rapamycin (20 nM) or a vehicle (-) was added to 293T cells overexpressing myc-PRAS40, and the levels of mTOR and raptor in myc immunoprecipitates were analyzed on immunoblots. (**f**) PRAS40 suppresses S6K1 phosphorylation in 293T cells transduced with tuberin shRNA. HA-S6K1 was expressed in 293T cells with or without myc-Ftagged PRAS40 and Rheb, and cell lysates analyzed for the phosphorylation state of S6K1 at Thr389. (**g**) PRAS40 overexpression suppresses S6K1 phosphorylation in 293T cells overexpressing Rheb. (**h**) PRAS40 suppresses the stimulatory effect of Rheb Q64L, a constitutively active mutant of Rheb, on the S6K1 phosphorylation. HEK293T cells were transfected with indicated plasmids and the phosphorylation state at Thr389 and expression level of S6K1 were analyzed by Western blotting.
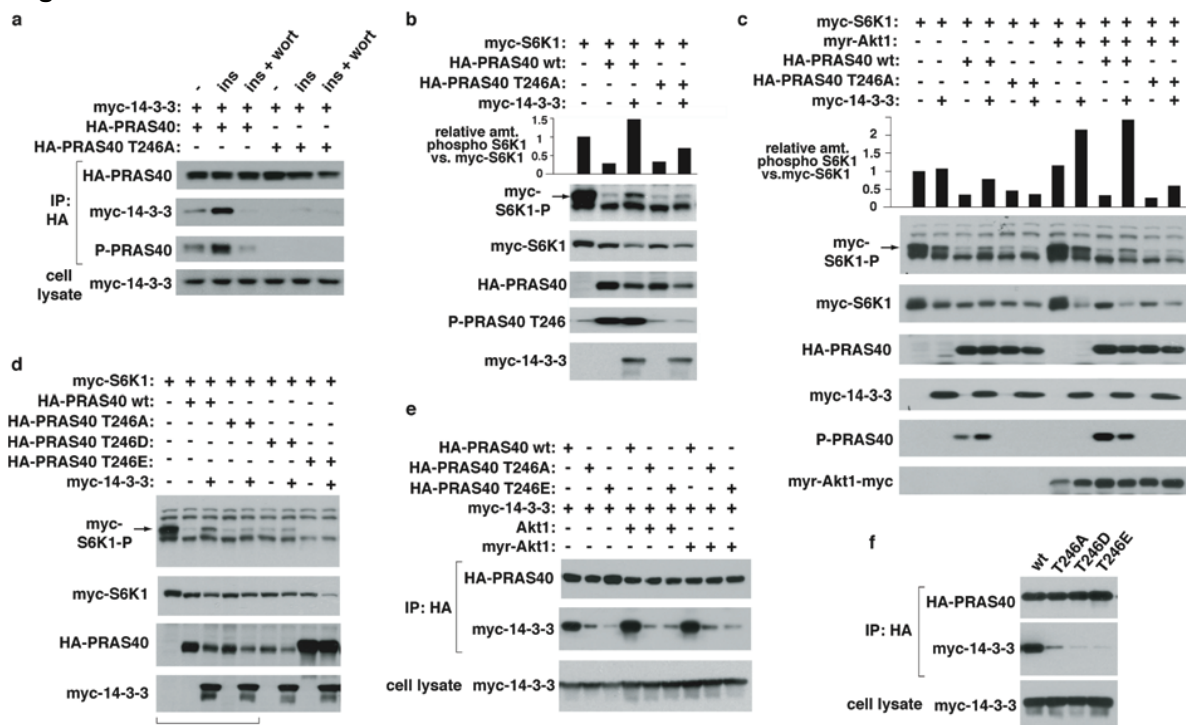
Figure S4

Figure S4. PRAS40 phosphorylation and binding to 14-3-3 are crucial for activation of mTOR signaling. (**a**) PRAS40 phosphorylation at Thr246 is stimulated by insulin and required for binding 14-3-3. 293T cells overexpressing myc-tagged 14-3-3 and either HA-tagged PRAS40 wild type or T246A mutant were starved of serum overnight and treated with insulin (100 nM) for 20 min. The amount of myc-14-3-3 bound to HA-PRAS40 in HA immunoprecipitates, the expression level of myc-14-3-3, and the phosphorylation state of PRAS40 at Thr246 were analyzed by Western blotting. (**b**) 14-3-3 relieves S6K1 phosphorylation from the inhibition by PRAS40. Indicated recombinant proteins were expressed in 293T cells and the phosphorylation states of S6K1 at Thr389 and PRAS40 at Thr246 were analyzed on immunoblots. (**c**) Synergetic effects of Akt and 14-3-3 on the recovery of S6K1 phosphorylation from PRAS40 inhibition. 293T cells were transfected with plasmids encoding the indicated proteins and 48 hrs post-transfection cell lysate was analyzed for the phosphorylation states and expression levels of the proteins. (**d**) PRAS40 T246A, T246E and T246D mutants do not have stimulatory effects on S6K1 phosphorylation. HA-tagged PRAS40 T246A, T246E or T246D mutant was expressed together with myc-S6K1 and/or Akt1, myr-Akt1, 14-3-3 in 293T cells, and the levels of phosphorylation of S6K1 at Thr389 and the expression levels of recombinant proteins were analyzed by immunoblotting. The data in the star-marked lanes are also shown in (b). (**e**) Akt or myr-Akt does not induce the interaction of T246A or T246E with 14-3-3. HA-tagged PRAS40 T246A or T246E was expressed with myc-14-3-3 and either Akt1 or myr-Akt1 in 293T cells. Two days post-transfection, the amount of myc-14-3-3 bound to HA-PRAS40 in HA immunoprecipitate, the levels of PRAS40 phosphorylated at Thr246, and the expression level of myc-14-3-3 were analyzed by Western blotting. (**f**) PRAS40 T246A, T246E and T246D are incapable of binding 14-3-3. HA-tagged PRAS40 T246A, T246E, or T246D was expressed together with myc-tagged 14-3-3 in 293T cells. The amount of myc-14-3-3 bound to HA-PRAS40 in HA immunoprecipitates and the expression level of myc-14-3-3 were analyzed by Western blotting.

Table 1. A list of peptide sequences matched with LTQ MS/MS data

P-scores	Mass (M+H)	Precursor Mass Error	Xcorr	ΔCn	Sp	Rank	# b and y ions detected (MS/MS)	# predicted b and y ions (MS/MS)	Matched Peptide Sequences
raptor									
0.9999	1158.3	(-0.0)	3.4984	0.474	903.4	1	16	20	K.ALETIGANLQK.Q
0.9991	1466.6	(+0.0)	3.1247	0.522	780.8	1	17	22	K.IPEEHDLESQIR.K
0.9992	1134.3	(-0.6)	3.4071	0.339	803	1	15	16	R.LDDQIFLNR.N
0.9593	1502.7	(+0.8)	1.9882	0.352	276.9	1	14	24	K.LYSLLSDPIPEVR.C
0.9997	2120.2	(-1.3)	5.3332	0.63	1991.2	1	35	76	K.MFDKGPEQTADDADDAAGHK.S
0.9925	2120.2	(+2.0)	5.7583	0.645	2736.5	1	38	76	K.MFDKGPEQTADDADDAAGHK.S
0.9997	2136.2	(+0.5)	4.6509	0.548	2245.2	1	37	76	K.M*FDKGPEQTADDADDAAGHK.S
0.999	1357.6	(+0.1)	3.7534	0.423	1974.1	1	19	22	R.MPESVNVLQIVK.G
0.9911	2148.4	(+1.8)	2.9445	0.387	269.5	2	15	36	K.NPEMVTAWQGLSDMLPTTR.G
0.9996	2181.6	(+0.7)	4.365	0.625	349.8	1	17	36	R.NPPEQLPIVLQVLLSQVHR.L
0.9733	1932.1	(-0.5)	1.8997	0.359	339.2	1	18	36	K.NYALPSPATTEGGSLTPVR.D
0.9927	1390.6	(+1.3)	2.8931	0.406	383.5	1	13	22	R.PTVNGEVWVFNK.N
0.9685	1258.5	(+1.1)	2.3733	0.299	457.7	1	17	24	R.SLIVAGLGDGSIR.V
0.999	1258.5	(-0.8)	4.1884	0.498	1917	1	21	24	R.SLIVAGLGDGSIR.V
0.9786	1390.6	(+0.2)	2.631	0.324	515.9	1	15	22	R.PTVNGEVWVFNK.N
GβL									
0.9689	2269.5	(-0.6)	4.2196	0.056	1013.3	1	21	38	R.MYDLNSNNPNPIISYDGVNK.N
0.998	1302.4	(-0.1)	2.9977	0.352	1175.3	1	17	22	K.NIASVGFHEDGR.W
0.9999	2038.2	(+0.5)	5.0321	0.558	2304.2	1	24	34	R.TVQHQDSQVNALEVTPDR.S
0.9995	2038.2	(-1.0)	3.4955	0.44	2222.8	1	26	34	R.TVQHQDSQVNALEVTPDR.S
rictor									
0.9999	1108.2	(+1.4)	2.9028	0.495	1287.8	1	18	20	R.LSDGFVAAEAK.T
0.9879	1308.5	(-0.1)	2.5881	0.257	1497.2	1	17	20	R.YLIQDSSILQK.V
0.9987	1655.8	(-0.3)	3.9651	0.444	1679.7	1	26	34	R.AFAHDAGGLPSGTGGLVK.N
0.9846	1813.9	(-0.3)	5.1911	0.658	1630.3	1	28	32	K.HIEDTGSTPSIGENDLK.F
0.988	1305.5	(-0.0)	2.2002	0.337	754.9	1	16	22	R.LVVESSTSSHMK.I
0.9982	1369.6	(+0.8)	3.1632	0.5	873.8	1	17	22	K.TLQLETSFMGNK.H
0.9846	1141.3	(+1.3)	2.1218	0.392	243.7	1	14	18	K.LTVSSLDYSR.D
Sin1									
0.9379	994.1	(+0.3)	2.2299	0.176	538.8	1	12	14	K.VNYILESR.A
0.9996	1728.9	(-0.1)	3.8725	0.599	870.9	1	20	30	R.INAAHGFSLIQVDNTK.V
1.0000	1212.4	(+1.3)	3.4983	0.434	1275.3	1	17	20	K.FGFSTLALVEK.Y
PRAS40									
0.992	1477.6	(-0.6)	2.436	0.335	431.7	1	16	24	R.EAEDTQVFGDLPR.P

Listed are peptide sequence matches with *P*-scores greater than 0.95 from the Sequest analysis of MS/MS data of mTOR immunoprecipitates.

Table 2. Cell size reduction by PRAS40 overexpression

cell types	DNA constructs[a]	diameter (μm) avg +/- std	relative cell volume (%)[b]
293T	null	15.31 +/- 0.26 (n=5)[c]	(100)
	PRAS40	15.07 +/- 0.21 (n=6)	(96.9)
EEF TSC2+/+	null	17.10 +/- 0.66 (n=8)	(100)
	PRAS40	16.57 +/- 0.79 (n=6)	(93.9)
EEF TSC2-/-	null	18.52 +/- 1.86 (n=8)[d]	(100)
	PRAS40	17.23 +/- 0.51 (n=10)[d]	(86.6)

[a]CSII-EF-MCS encoding myc-PRAS40 or the vector only (null) was transduced into the cells through lentiviral infection. [b]Relative cell volume in percent compared to volumes of cells transduced with null lentiviral vector. Approximately 5,000 and 800 cells were analyzed for 293T and TSC cells per measurement, respectively. [c]The number of measurements of cell sizes. [d]p=0.05 from the Student t-test.